C. S. Jacobs et al.: X/Ka Celestial Frame Improvements: Vision to Reality, IVS 2010 General Meeting Proceedings, p.285–289
http://ivscc.gsfc.nasa.gov/publications/gm2010/jacobs1.pdf

X/Ka Celestial Frame Improvements: Vision to Reality

C. S. Jacobs [1], *D. S. Bagri* [1], *M. J. Britcliffe* [1], *J. E. Clark* [1], *M. M. Franco* [1], *C. Garcia-Miro* [2], *C. E. Goodhart* [1], *S. Horiuchi* [3], *S. T. Lowe* [1], *V. E. Moll* [2], *R. Navarro* [1], *S. P. Rogstad* [1], *R. C. Proctor* [1], *E. H. Sigman* [1], *L. J. Skjerve* [1], *M. A. Soriano* [1], *O. J. Sovers* [1], *B. C. Tucker* [1], *D. Wang* [1], *L. A. White* [1]

[1)] *Jet Propulsion Laboratory, California Institute of Technology/NASA*
[2)] *Ingenieria y Servicios Aeroespaciales, Instituto Nacional de Técnica Aeroespacial/NASA*
[3)] *C.S.I.R.O. Astronomy and Space Science/NASA*

Contact author: C. S. Jacobs, e-mail: Christopher.S.Jacobs@jpl.nasa.gov

Abstract

In order to extend the International Celestial Reference Frame from its S/X-band (2.3/8.4 GHz) basis to a complementary frame at X/Ka-band (8.4/32 GHz), we began in mid-2005 an ongoing series of X/Ka observations using NASA's Deep Space Network (DSN) radio telescopes. Over the course of 47 sessions, we have detected 351 extra-galactic radio sources covering the full 24 hours of right ascension and declinations down to −45 degrees. Angular source position accuracy is at the part-per-billion level.

We developed an error budget which shows that the main errors arise from limited sensitivity, mismodeling of the troposphere, uncalibrated instrumental effects, and the lack of a southern baseline. Recent work has improved sensitivity by improving pointing calibrations and by increasing the data rate four-fold. Troposphere calibration has been demonstrated at the mm-level. Construction of instrumental phase calibrators and new digital baseband filtering electronics began in recent months. We will discuss the expected effect of these improvements on the X/Ka frame.

1. Introduction

For over three decades, radio frequency work in global astrometry, geodesy, and deep space navigation has been done at S/X-band (2.3/8.4 GHz) [10]. This well known work has been tremendously successful in producing sub-100 μas level global astrometry (e.g.[7]) and sub-cm geodesy. Less well known is that at the same time when S/X work started—the late 1970s—visionary colleagues, e.g. [2, 8], started to lay the foundation for one day doing X/Ka-band (8.4/32 GHz) VLBI. Only now, in the last decade, have technological and programmatic developments allowed that vision to blossom. This paper will report on the current status of X/Ka-band VLBI, present our plan for improving X/Ka-band astrometry, and assess our progress towards realizing that plan.

Ka-band pros: Increasing observing frequencies by a factor of four promises several advantages. For the Deep Space Network, the chief driver is the potential for higher telemetry rates to space probes. Other advantages include 1) sources become more compact lending hope that the positions will be more stable over time, 2) radio frequency interference at S-band would be avoided, 3) Ionosphere and solar plasma effects on delay and signal coherence are reduced about ∼15-fold.

Ka-band cons: While these are significant advantages, there are also disadvantages. The change from 2.3/8.4 GHz to 8.4/32 GHz moves one closer to the water vapor line at 22 GHz and thus increases the system temperature to 6–15 Kelvins per atmosphere or more, thereby increasing weather sensitivity. Many sources become weaker and/or resolved. Coherence times are shortened so that practical integration times are a few minutes or less—even in relatively dry climates.

Antenna pointing accuracy must be tightened by the factor-of-4 wavelength reduction. These effects all combine to lower the system sensitivity. Thus counter-measures are needed.

This paper is organized as follows: We will briefly review present X/Ka-band astrometry including an estimate of its accuracy based on comparison to the S/X-band ICRF2. A simplified error budget consisting of errors from sensitivity limitations, instrumental errors, and troposphere mismodeling will guide our discussion of plans for reducing each of those error sources. We will emphasize how our vision for reducing errors is becoming a reality.

2. Observations and Current Accuracy

The results presented here are from 47 Very Long Baseline Interferometry (VLBI) observing sessions of 24 hour duration done from July 2005 until December 2009 using NASA's Deep Space Stations (DSS) 25 or 26 in Goldstone, California to either DSS 34 in Tidbinbilla, Australia or DSS 55 outside Madrid, Spain to form interferometric baselines of 10,500 and 8,400 km length, respectively.

We recorded simultaneous X (8.4 GHz) and Ka-band (32 GHz), sampling each band at 56 Mbps. Each band's 7 channels (each ±2 MHz) spanned a bandwidth of ≈360 MHz. For the three most recent sessions, the data rates were doubled to 224 Mbps—split between bands as 80/144 Mbps.

In all, we detected 351 extragalactic radio sources which covered the full 24 hours of RA and declinations down to −45°. In Figure 1, these sources are plotted using an Aitoff projection to show their locations on the sky. Note that the declination precision decreases as one moves toward the south. This is a result of having significantly less data on the California to Australia baseline combined with the need to observe sources closer to the horizon as declination moves south, thus incurring greater error from higher system temperatures and tropospheric mismodeling.

An external estimate of the accuracy of our astrometry was made by comparing X/Ka source positions to the S/X-based ICRF2 [7]. For 323 common sources, the weighted RMS (wRMS) differences are 190 μas in RA cos(dec) and 265 μas in declination [5]. Examination of the differences revealed decreasing accuracy in RA and declination as one moves southward (see Fig. 1).

3. Error Budget: Sensitivity, Instrumentation, Troposphere

Having presented the number, spatial distribution, and accuracy of our source positions, we now discuss the major errors currently limiting X/Ka accuracy. The median delay thermal error was ≈ 45 psec. Fig. 2's plot of data scatter vs. the nominal SNR sheds light on the error budget. For SNRs < 15 dB the thermal error dominates. For higher SNRs, the data scatter is limited by a noise floor caused by tropospheric and instrumental errors. Let's now look in more detail at these three main errors: SNR, instrumentation, and troposphere.

Sensitivity: Relative to S and X-bands, Ka-band has higher system temperatures, worse pointing, and larger coherence losses, all of which lower sensitivity and increase delay scatter. Much work was done to minimize signal loss due to mis-pointing, resulting in recovery of roughly +3 dB gain in our Ka-band sensitivity [9].

Fortunately, it is feasible and affordable to further increase sensitivity by increasing the recorded bit rate using recent advances [11]. Thus, while most of the X/Ka data presented in this paper used the same 112 Mbps recording rate as used in much previous S/X work, we have recently

begun to leverage the Mark 5A system's potential by recording at 448 Mbps (Fig. 3). We plan to use 896 Mbps (split as 320/576 Mbps) within the next year, thereby improving the SNR by a factor of 3.2 which would reduce the median thermal errors to ≈ 15 psec—below the instrumental and tropospheric floor! Within 2–3 years, deployment of Mark 5C recorders is expected to increase maximum data rates from 1024 Mbps to 4096 Mbps [11] thereby further improving sensitivity.

Instrumentation: A prototype Ka-band phase calibrator [3] based on A.E.E. Rogers's tunnel diode concept revealed approximately diurnal instrumental effects with ≈180 psec amplitude (see Fig. 4). Although the VLBI data have been used to partially parameterize these effects, in order to achieve better than 200 μas accuracy in a timely manner, we have begun building operational calibrators for deployment within the next few years. Fig. 5 shows our first production unit.

Further instrumental improvements are expected from replacing aging Mark IV video converters with Digital Back Ends (DBE). The DBE's phase-linear Finite Impulse Response (FIR) filters will reduce phase errors and increase the spanned bandwidth from 360 to 500 MHz thus reducing both systematic and random group delay errors.

Troposphere: Work started in the 1990s led to JPL's Advanced WVR (A-WVR) which demonstrated the ability to calibrate tropospheric delay fluctuations on inter-continental baselines with 1 mm accuracy [4, 1]. Recent work has focussed on modifying commercial designs to retain mm-level accuracy while being smaller and lighter so as to enable the WVR to be mounted on the VLBI subreflector. This will improve beam alignment and automate co-pointed observing.

4. Conclusions

The S/X-band ICRF has now been extended to the four times higher frequency of X/Ka-band (8.4/32 GHz). A total of 351 sources have been successfully detected. For the 323 sources with sufficient observations to warrant comparison to the ICRF2's S/X results, the wRMS positional agreement was 190 μas in RA cos(declination) and 265 μas in declination.

Our current limiting errors are SNR, lack of instrumental calibration, and troposphere mismodeling. SNR errors are being reduced by improving pointing and increasing the data rate. Instrumental errors will be reduced by phase calibrators and DBEs being built for deployment within the next few years. We are working to make mm-level WVR troposphere calibration less expensive and lighter weight to enable its operational use. If all these improvements are achieved, we expect 200 μas or better accuracy within a few years.

5. Acknowledgements

The research described herein was performed at the Jet Propulsion Laboratory of the California Institute of Technology, under a contract with the National Aeronautics and Space Administration.

References

[1] Bar-Sever et al, 'Atmospheric Media Calibration for the Deep Space Network,' Proc. IEEE (Special issue), 95, 11, Nov. 2007. http://ieeexplore.ieee.org/stamp/stamp.jsp?arnumber=04390031

[2] deGroot, N.F., 'Ka-band (32 GHz) Allocations for Deep Space,' TDA Prog. Rept. 42-88, pp. 104–109. 15 Feb 1987. http://tmo.jpl.nasa.gov/progress_report/42-88/88N.PDF

[3] Hammel, Tucker, & Calhoun, 'Phase Cal. Generator,' IPN Prog. Rep. 42-154, Pasadena, CA, 2003. http://tmo.jpl.nasa.gov/progress_report/42-154/154H.pdf

[4] Jacobs et al, 'Improving Astrometric VLBI by using WVR Calibrations,' BAAS, 36, 5, 2004. http://www.aas.org/publications/baas/v36n5/aas205/716.htm

[5] Jacobs & Sovers, 'X/Ka-band Global Astrometric Results,' Proc. 19th EVGA, Bordeaux, France, 2009. http://www.u-bordeaux1.fr/vlbi2009/proceedgs/03_Jacobs.pdf

[6] Ma *et al*, 'The ICRF as Realized by VLBI,' AJ, 116, 1, 516–546, Jul 1998. doi: 10.1086/300408 http://iopscience.iop.org/1538-3881/116/1/516/

[7] Ma et al, 'The 2nd Realization of the ICRF by VLBI,' IERS, Frankfurt, Germany, Oct. 2009. http://www.iers.org/nn_11216/IERS/EN/Publications/TechnicalNotes/tn35.html

[8] Potter. P.D., 'Use of Ka-band for Radio Metric Determination,' NASA TDA Prog. Rept. 42-58, pp. 59–66, 15 Aug 1980. http://tmo.jpl.nasa.gov/progress_report/42-58/58N.PDF

[9] Rochblatt, D., P. Richter, P Withington, M. Vazquez, and J. Calvo, 'New Antenna Calibration Techniques in the Deep Space Network,' NASA JPL IPN Progress Report, 42-169, pp. 1–34, 15 May 2007. http://tmo.jpl.nasa.gov/progress_report/42-169/169A.pdf

[10] Sovers, Fanselow, & Jacobs, 'Astrometry, Geodesy with Radio Interferometry: Expts., Models, Results,' Rev. Mod. Phys., 70, 4, 1393–1454, Oct. 1998. http://link.aps.org/doi/10.1103/RevModPhys.70.1393

[11] Whitney, Ruszczyk, Romney, & Owens, 'Mark 5C VLBI Data System,' this volume, 2010. ftp://ivscc.gsfc.nasa.gov/pub/general-meeting/2010/presentations/GM2010_S5T01_whitney.pdf

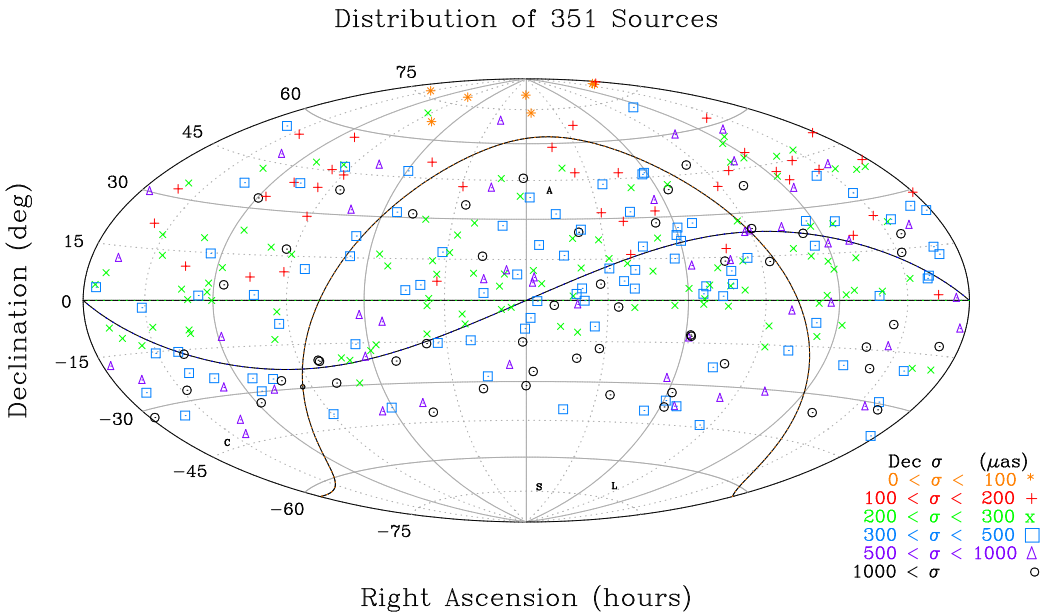

Figure 1. Distribution of 351 X/Ka-band sources detected to date. Symbols indicate 1-σ formal declination uncertainties as defined in the legend at lower right. $(\alpha, \delta) = (0, 0)$ is at the center. The ecliptic plane is indicated by the sinusoidal line. The galactic plane is indicated by the Ω-shaped line. Note the trend for decreasing declination precision moving southward. Local galactic neighborhoods indicated by A, C, S, L: Andromeda, Centaurus-A, Small & Large Magellanic clouds (none observed at X/Ka).

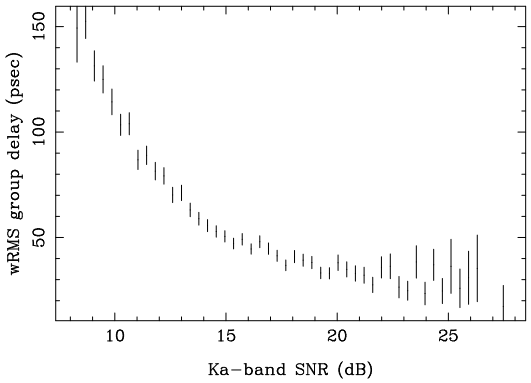

Figure 2. The wRMS residual group delay vs. Ka-band SNR. Thermal error dominates the VLBI residuals for SNR < 15 dB. As SNR increases past that point, a noise floor of $\approx$30 psec from tropospheric and instrumental errors is asymptotically approached.

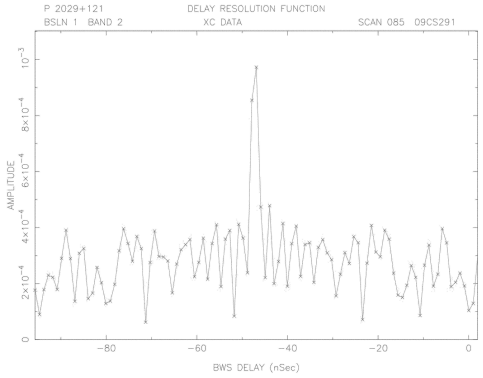

Figure 3. The first 448 Mbps fringes at X/Ka-band using the DSN: Day 291 of 2009, Goldstone to Madrid baseline using source P 2029+121 (one of several sources detected).

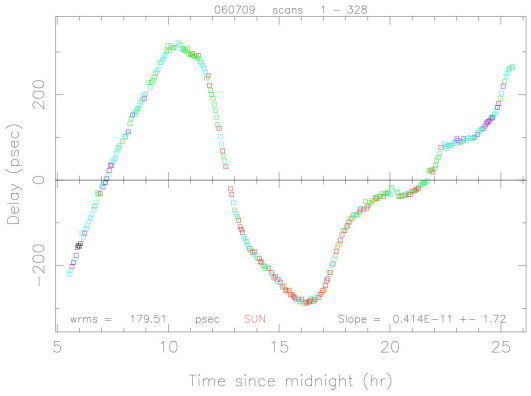

Figure 4. Ka-band proto-type phase calibrator group delays vs. time from 9 Jul 2006. Diurnal variation is driven by thermal changes in cables and other instrumentation. Color code indicates the sun angle (in order closest to farthest: orange, red, green, cyan, purple, black).

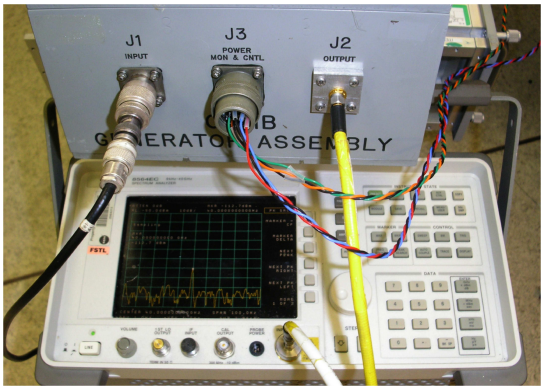

Figure 5. The first production Ka-band Phase Calibrator being tested on a spectrum analyzer. The calibration pulses are generated using a tunnel diode allowing operation up to 32 GHz. Design by Hammel, Tucker, & Calhoun (2003) based on a concept by A.E.E. Rogers.